J. Fluid Mech. (1974), *vol.* 63, *part* 3, *pp.* 607–622
Printed in Great Britain

Hydromechanics of low-Reynolds-number flow. Part 1. Rotation of axisymmetric prolate bodies

By ALLEN T. CHWANG AND T. YAO-TSU WU
Engineering Science Department, California Institute of Technology, Pasadena

(Received 1 May 1973)

The present series of studies is concerned with low-Reynolds-number flow in general; the main objective is to develop an effective method of solution for arbitrary body shapes. In this first part, consideration is given to the viscous flow generated by pure rotation of an axisymmetric body having an arbitrary prolate form, the inertia forces being assumed to have a negligible effect on the flow. The method of solution explored here is based on a spatial distribution of singular torques, called rotlets, by which the rotational motion of a given body can be represented.

Exact solutions are determined in closed form for a number of body shapes, including the dumbbell profile, elongated rods and some prolate forms. In the special case of prolate spheroids, the present exact solution agrees with that of Jeffery (1922), this being one of very few cases where previous exact solutions are available for comparison. The velocity field and the total torque are derived, and their salient features discussed for several representative and limiting cases. The moment coefficient $C_M = M/(8\pi\mu\omega_0 ab^2)$ (M being the torque of an axisymmetric body of length $2a$ and maximum radius b rotating at angular velocity ω_0 about its axis in a fluid of viscosity μ) of various body shapes so far investigated is found to lie between $\frac{2}{3}$ and 1, usually very near unity for not extremely slender bodies.

For slender bodies, an asymptotic relationship is found between the nose curvature and the rotlet strength near the end of its axial distribution. It is also found that the theory, when applied to slender bodies, remains valid at higher Reynolds numbers than was originally intended, so long as they are small compared with the (large) aspect ratio of the body, before the inertia effects become significant.

1. Introduction

In physical and biological science, and in engineering, there is a wide range of problems of interest concerning the flow of a viscous fluid in which a solitary or a large number of bodies of microscopic scale are moving, either being carried about passively by the flow, such as solid particles in sedimentation, or moving actively as in the locomotion of micro-organisms. In the case of suspensions containing small particles, the presence of the particles will influence the bulk properties of the suspension, which is a subject of general interest in rheology. In the motion of micro-organisms, the propulsion velocity depends critically

on their body shapes and modes of motion, as evidenced in the flagellar and ciliary movements and their variations.

A common feature of these flow phenomena is that the motion of the small objects relative to the surrounding fluid has a small characteristic Reynolds number Re. Typical values of Re may range from order unity, for sand particles settling in water, for example, down to 10^{-2}–10^{-6}, for various micro-organisms. In this low range of Reynolds numbers, the inertia of the surrounding fluid becomes insignificant compared with viscous effects and is generally neglected. The Stokes-flow problem so formulated is usually very difficult; not many exact or even approximate solutions are available except for the simplest body shapes, such as the sphere, ellipsoids and elongated rods (see, for example, Lamb 1932; Happel & Brenner 1965; Batchelor 1967, § 4.9).

In the limiting case of elongated bodies, which is especially important in flagellar propulsion, the theoretical development based on the same simplification (as stated above) has led to the so-called 'resistive theory' (see Lighthill 1969). This simple theory states that the force between a small longitudinal segment of a body and the surrounding fluid is resistive and viscous in origin, depending primarily on the instantaneous value of the velocity of that body section relative to its surrounding fluid. The resistive theory of propulsion was first considered by Hancock (1953), subsequently developed by Gray & Hancock (1955) for planar wave motions of an elongated cylinder and later extended by Chwang & Wu (1971, 1974) to include the angular momentum for helical movements of flagella. For the general case of bodies of arbitrary shape, however, only the asymptotic behaviour of the flow field at large distances has been discussed (see, for example, Oseen 1927; Lagerstrom 1964; Batchelor 1967); the details of an exact or approximate solution near a given body are nevertheless still required for the determination of the force and torque on the body in question.

The purpose of the present series of studies is to develop an effective method by which a number of exact solutions can be determined for both the rotational and translational motion of axisymmetric bodies with shapes covering several categories that can be easily extended to arbitrary-form computations. The method is based on a spatial distribution of singular forces (Stokeslets), torques (rotlets) and other types of flow singularities (doublets, stresslets, etc.) for possible representation of given motion of a solid. In comparison with classical methods for boundary-value problems, this method appears to be more powerful since it does not depend so critically on an optimum choice of co-ordinate system, or on a possible separation of variables, as in the boundary-problem approach. It is hoped that these exact solutions will guide approximate theories in general.

This first part of the series deals with the rotational motion of a class of axisymmetric bodies, including dumbbell-shaped bodies, elongated rods and certain prolate forms. Exact solutions have been determined in closed form for these cases. Of particular significance is the special case of prolate ellipsoids of revolution since this is a rare case where exact solutions of Edwardes (1892) and Jeffery (1922), both solutions being based on the boundary-value method, are available for comparison. The translational motion of bodies of arbitrary form will be analysed in a future part.

2. Vortical flow at low Reynolds number with solenoidal forces

The class of incompressible viscous flows to be considered here is characterized by the features that (i) inertial effects are negligible at sufficiently low Reynolds numbers, and (ii) the external forcing function, $\mathbf{F}(\mathbf{x})$ say, is solenoidal, that is

$$\nabla.\mathbf{F} = 0, \tag{1}$$

$\mathbf{x}$ being the position vector in a three-dimensional Euclidean space E_3, which is taken to be unbounded. The flow velocity $\mathbf{u}(\mathbf{x})$ and pressure $p(\mathbf{x})$ then satisfy the Stokes equations

$$\nabla.\mathbf{u} = 0, \tag{2}$$

$$\nabla p = \mu\nabla^2\mathbf{u} + \mathbf{F}(\mathbf{x}), \quad \mathbf{F}(\mathbf{x}) = 4\pi\mu\nabla\times\boldsymbol{\Omega}(\mathbf{x}), \tag{3}$$

where μ is the constant viscosity coefficient and $\mathbf{F} = 4\pi\mu\nabla\times\boldsymbol{\Omega}$ is the extraneous force per unit volume of E_3, now specified in terms of a vector potential $\mu\boldsymbol{\Omega}$ ($\boldsymbol{\Omega}$ having the dimensions of vorticity). We further require that

$$|\mathbf{u}| \to 0, \quad p \to p_\infty \quad \text{as} \quad |\mathbf{x}| \to \infty. \tag{4}$$

The general purpose here is to seek the flow $\mathbf{u}$ due to possible rotation of a solid body that can be represented by a distribution of potentials $\boldsymbol{\Omega}(\mathbf{x})$.

The pressure corresponding to the class of solenoidal forces is seen to be harmonic and regular in the entire space, since by taking the divergence of (3) and making use of (2),

$$\nabla^2 p = 0 \quad (0 \leqslant |\mathbf{x}| \geqslant \infty),$$

and hence, by the well-known theorem for harmonic functions (see Kellogg 1929, chap. 8),

$$p = p_\infty = \text{constant}. \tag{5}$$

We note that (5) may no longer be valid when the flow is bounded by additional material surfaces (e.g. a wall); such flows generally require consideration of other types of forces and flow singularities (see Blake & Chwang 1974).

The case of fundamental importance is when $\boldsymbol{\Omega}$ has a point singularity at the origin:

$$\boldsymbol{\Omega}(\mathbf{x}) = \boldsymbol{\gamma}\delta(\mathbf{x}), \tag{6}$$

$\boldsymbol{\gamma}$ being a constant vector and $\delta(\mathbf{x})$ the three-dimensional Dirac delta-function. The corresponding velocity, by virtue of (5), satisfies the equation

$$\nabla^2\mathbf{u} = -4\pi\nabla\times(\boldsymbol{\gamma}\delta(\mathbf{x})), \tag{7}$$

which clearly has the solution

$$\mathbf{u} = \nabla\times\left(\frac{\boldsymbol{\gamma}}{R}\right) = \frac{\boldsymbol{\gamma}\times\mathbf{x}}{R^3} \quad (R = |\mathbf{x}|). \tag{8}$$

This solution is called a 'rotlet'; it is also called a 'couplet' by Batchelor (1970). The rotlet also results from an antisymmetric contraction of a Stokes-doublet (e.g. see Blake & Chwang 1974). The vorticity associated with the rotlet is readily deduced to be

$$\boldsymbol{\zeta} = \nabla\times\mathbf{u} = -\frac{\boldsymbol{\gamma}}{R^3} + \frac{3(\boldsymbol{\gamma}.\mathbf{x})\,\mathbf{x}}{R^5}. \tag{9}$$

This vorticity field is seen to be completely analogous to the velocity of a potential doublet of strength $\boldsymbol{\gamma}$; the vortex lines of a rotlet therefore resemble the streamlines of an isolated dipole (of equal magnitude).

Physically, (8) provides the velocity generated by a sphere of radius a rotating about the $\boldsymbol{\gamma}$ axis with angular velocity $\omega_0 = \gamma/a^3$, where $\gamma = |\boldsymbol{\gamma}|$, since it satisfies the boundary condition $\mathbf{u} = \boldsymbol{\omega}_0 \times \mathbf{x}$ on $R = a$. The characteristic Reynolds number, based on the reference velocity at the equator, is small when

$$Re = \omega_0 a^2/\nu = \gamma/a\nu \ll 1, \tag{10}$$

where ν is the kinematic viscosity. This condition ensures that inertial effects remain insignificant for $R \geqslant a$.

The torque exerted on the rotlet (or equivalently, on the sphere of radius a) by the surrounding fluid is

$$\mathbf{M} = -\int_{R=a} \mathbf{x} \times (\boldsymbol{\sigma}\mathbf{n})\, dS = -8\pi\mu\boldsymbol{\gamma} \quad (= -8\pi\mu a^3 \boldsymbol{\omega}_0), \tag{11}$$

where $\mathbf{n}$ is the unit outward normal at the surface element dS and $\boldsymbol{\sigma}$ is the stress tensor. On the other hand, the net force acting on the rotlet (or on the rotating sphere), is seen, on account of the axial symmetry, to be zero.

For a volume distribution of rotlets $\boldsymbol{\Omega}(\mathbf{x})$, the solution can be constructed by linear superposition as

$$\mathbf{u} = \nabla \times \mathbf{A}, \quad \mathbf{A}(\mathbf{x}) = \int_V \frac{\boldsymbol{\Omega}(\mathbf{x}')}{|\mathbf{x}-\mathbf{x}'|}\, d^3x', \tag{12}$$

where V denotes either a finite region or an infinite subspace of E_3 that encloses an appropriate distribution of $\boldsymbol{\Omega}$'s. Here the velocity $\mathbf{u}$ has a vector potential $\mathbf{A}$. The vorticity field, by superposition of distributions like (9), becomes

$$\boldsymbol{\zeta}(\mathbf{x}) = \int_V \left\{ -\frac{\boldsymbol{\Omega}(\mathbf{x}')}{|\mathbf{x}-\mathbf{x}'|^3} + 3(\mathbf{x}-\mathbf{x}')\frac{(\mathbf{x}-\mathbf{x}')\cdot\boldsymbol{\Omega}(\mathbf{x}')}{|\mathbf{x}-\mathbf{x}'|^5} \right\} d^3x'. \tag{13}$$

The total torque exerted on the system of rotlets $\boldsymbol{\Omega}(\mathbf{x})$ by the fluid, according to (11) and (6), is

$$\mathbf{M} = -8\pi\mu \int_V \boldsymbol{\Omega}(\mathbf{x})\, d^3x. \tag{14}$$

Using this line of approach, the viscous flow generated by a wide class of axisymmetric bodies rotating about their axes of symmetry can be represented by an axial distribution of rotlets. In terms of the cylindrical polar co-ordinates (x, r, θ), the body shape is prescribed as

$$r = r_0(x) \quad (-a \leqslant x \leqslant a, \quad r_0(\pm a) = 0). \tag{15}$$

We seek the representation of the body rotation about the x axis, with angular velocity ω_0, by an axial distribution of rotlets of the form (see figure 1)

$$\boldsymbol{\Omega} = \mathbf{e}_x \Gamma(x)\, \delta(y)\, \delta(z) \quad (-c_1 \leqslant x \leqslant c_2), \tag{16}$$

where $(\mathbf{e}_x, \mathbf{e}_r, \mathbf{e}_\theta)$ are the base vectors, $\Gamma(x)$ is the line distribution and c_1 and c_2 are two constants $(c_1, c_2 \leqslant a)$. (Obviously, $c_1 = c_2 = c$ say, for bodies with

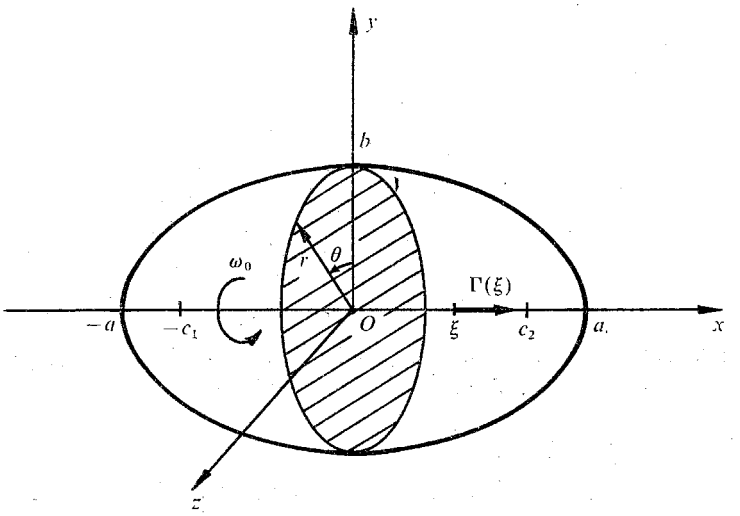

FIGURE 1. Line distribution of rotlets of strength $\Gamma(x)$ along the x axis in $-c_1 < x < c_2$, representing an axisymmetric body rotating with angular velocity ω_0 about the x axis. The body shape shown has the fore-and-aft symmetry, with $\Gamma(-x) = \Gamma(x)$ and $c_1 = c_2 = c$.

fore-and-aft symmetry, i.e. when $r_0(x) = r_0(-x)$.) The corresponding velocity, by (12), has only a θ component: $\mathbf{u} = (0, 0, u_\theta)$, where

$$u_\theta = r \int_{-c_1}^{c_2} \frac{\Gamma(\xi)\, d\xi}{[R(x-\xi, r)]^3}, \quad R(x,r) = (x^2+r^2)^{\frac{1}{2}}. \tag{17}$$

The no-slip condition, requiring $u_\theta(x, r_0(x)) = \omega_0 r_0(x)$, now becomes

$$F(x,r) \equiv \int_{-c_1}^{c_2} \frac{\Gamma(\xi)\, d\xi}{R^3(x-\xi, r)} = \omega_0 \quad (r = r_0(x), \quad |x| \leqslant a). \tag{18}$$

For the 'direct problem' with a specified body profile $r_0(x)$ and angular velocity ω_0, (18) is a Fredholm integral equation (of the first kind) for the rotlet strength $\Gamma(x)$ and the parameters c_1 and c_2. For the 'inverse problem', (18) directly provides the body-shape function $r_0(x)$ for given rotlet distribution $\Gamma(x)$ and parameters c_1 and c_2. Below we shall limit our discussion to rigid-body rotations, or $\omega_0 =$ constant, although the general case with a differential rotation of a given body can still be treated within the same framework.

The net torque exerted by the fluid on the rotating body represented by the rotlet distribution (16), according to (14), is $\mathbf{M} = -\mathbf{e}_x M$, where

$$M = 8\pi\mu \int_{-c_1}^{c_2} \Gamma(x)\, dx. \tag{19}$$

This result can also be obtained by integrating the torque $-2\pi r_c^2 \tau_{r\theta}(x, r_c)$ over a control surface $r = r_c > \max[r_0(x)]$, from $x = -\infty$ to ∞, $\tau_{r\theta} = \mu r \partial(u_\theta/r)/\partial r$ being the azimuthal component of the shear stress tensor.

We now proceed to discuss a few relatively simple, yet representative cases of rotlet distributions, some posed as inverse and some as direct problems.

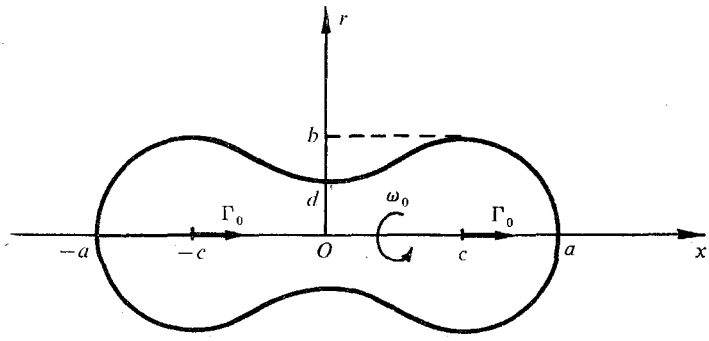

FIGURE 2. A class of dumbbell-shaped bodies in rotation that can be represented by a pair of isolated rotlets.

3. Dumbbell-shaped bodies

As in the construction of Rankine bodies in potential flow by employing isolated sources and sinks, we take two isolated rotlets of equal strength (see figure 2),

$$\Gamma(x) = \tfrac{1}{2}\Gamma_0\delta(x+c) + \tfrac{1}{2}\Gamma_0\delta(x-c), \tag{20}$$

for which the boundary condition (18) becomes

$$R_1^{-3} + R_2^{-3} = 2\omega_0/\Gamma_0 \quad (r = r_0(x), \quad |x| \leqslant a), \tag{21}$$

where

$$R_1 = [(x+c)^2 + r^2]^{\frac{1}{2}}, \quad R_2 = [(x-c)^2 + r^2]^{\frac{1}{2}}. \tag{22}$$

At the terminal points ($x = \pm a, r_0 = 0$) and at the dumbbell neck ($x = 0$, $r_0 = d$ say) condition (21) reduces, respectively, to

$$a(a^2 + 3c^2)(a^2 - c^2)^{-3} = \omega_0/\Gamma_0, \tag{23a}$$

$$(c^2 + d^2)^{-\frac{3}{2}} = \omega_0/\Gamma_0. \tag{23b}$$

Elimination of ω_0/Γ_0 between (23a, b) yields

$$(a^2 - c^2)^3 = a(a^2 + 3c^2)(c^2 + d^2)^{\frac{3}{2}}, \tag{24}$$

which provides a relationship between the geometric parameters c/a and d/a. The same elimination between (21) and (23a) results in an algebraic equation which determines the shape function $r_0/a = f(x/a; c/a)$, which depends on one geometric parameter, c/a.

The total torque acting on the dumbbell, by (19), (20) and (23), is

$$M = 8\pi\mu\Gamma_0 = 8\pi\mu\omega_0(c^2 + d^2)^{\frac{3}{2}}. \tag{25}$$

This torque is equal to that on a sphere (rotating with the same ω_0, see (11)) of an equivalent radius $a_e = (c^2 + d^2)^{\frac{1}{2}}$, which is the distance between the focal point ($x = c$, $r = 0$) and the neck centre ($x = 0$, $r = d$). To facilitate a uniform comparison with other cases to be discussed later, we define the torque coefficient C_M with reference to $8\pi\mu\omega_0 ab^2$, where b is the maximum radial extent, that is $b = \max[r_0(x)]$ as determined from (21). Thus, for the dumbbell,

$$C_M \equiv \frac{M}{8\pi\mu\omega_0 ab^2} = \frac{1}{ab^2}(c^2 + d^2)^{\frac{3}{2}}. \tag{26}$$

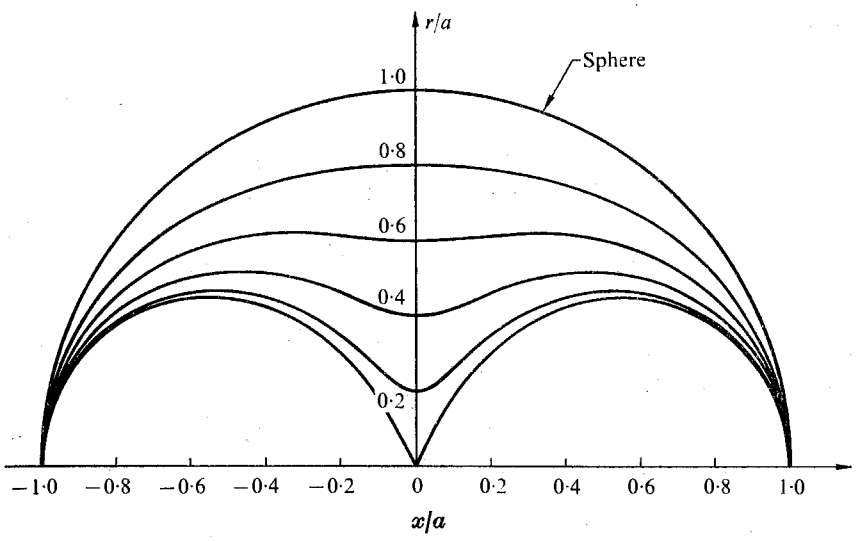

FIGURE 3. Some axisymmetric body shapes generated by a pair of rotlets. The numbers along the r/a axis designate the geometric parameter d/a.

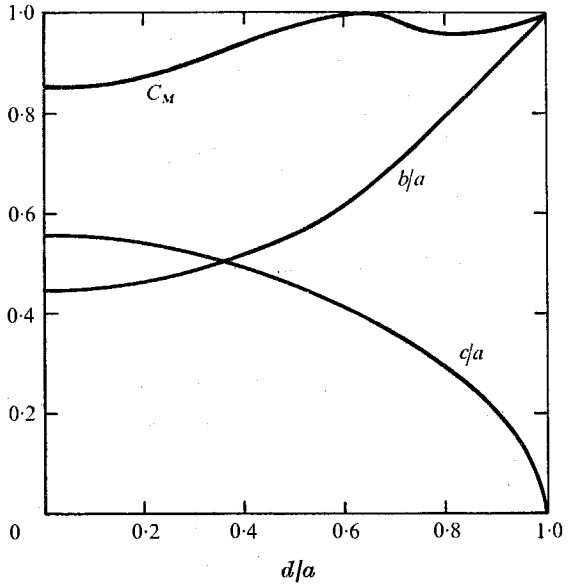

FIGURE 4. Variation of the moment coefficient $C_M = M/8\pi\mu\omega_0 ab^2$, the ratio b/a of the maximum radius to the body length and the ratio c/a of the range of rotlet distribution to the body length *vs.* the parameter d/a for the class of bodies shown in figure 3.

Several body profiles are shown in figure 3 for various d/a. The corresponding torque coefficient C_M, the maximum-thickness-to-length ratio b/a and the rotlet spacing c/a, as computed from (26), (21) and (24), are shown in figure 4 over the range $0 \leqslant d/a \leqslant 1$, within which the body remains in one piece. When the rotlet pair coalesces in the limit of vanishing c, the body becomes a sphere of radius a (hence $b = d = a$), giving the sphere result: $C_M = 1$. As d/a decreases from 1,

c/a increases monotonically to 0·556 at $d = 0$, b/a decreases to 0·449, while C_M remains in the range $0{\cdot}85 < C_M \leqslant 1$. This result for C_M further indicates, according to the definition (26), that the torque M is roughly equal to $8\pi\mu\omega_0 ab^2$, within a maximum error of 15 %.

For $c/a > 0{\cdot}556$, the rotlets then become so far apart that a body composed of two separate pieces results, approaching the state of two isolated spheres as $c/a \to 1$. In all these cases the sum of b/a and c/a is nearly unity, signifying that the rotlets are located approximately at the points where r_0 is maximum.

4. Uniform axial distribution of rotlets

We consider next the uniform distribution

$$\Gamma(x) = \beta_0 = \text{constant} \quad (|x| \leqslant c). \tag{27}$$

The corresponding boundary condition (see (18)) can be integrated to yield

$$B_0(x, r; c) \equiv \frac{1}{r^2}\left[\frac{x+c}{R_1} - \frac{x-c}{R_2}\right] = \frac{\omega_0}{\beta_0} \quad (r = r_0(x), \quad |x| \leqslant a), \tag{28}$$

where R_1 and R_2 are given by (22). For the semi-major axis ($x = a$, $r = 0$) and semi-minor axis ($x = 0$, $r = b$) in particular, (28) yields the relations

$$2ac(a^2 - c^2)^{-2} = \omega_0/\beta_0, \tag{29a}$$

$$2cb^{-2}(b^2 + c^2)^{-\frac{1}{2}} = \omega_0/\beta_0. \tag{29b}$$

Hence,

$$(a^2 - c^2)^2 = ab^2(b^2 + c^2)^{\frac{1}{2}}, \tag{29c}$$

which relates the parameters b/a and c/a. The shape function $r_0 = r_0(x; a, c)$ is then given by (28) and (29).

The torque corresponding to the uniform distribution is simply

$$M = 16\pi\mu c\beta_0 = 8\pi\mu\omega_0 b^2(b^2 + c^2)^{\frac{1}{2}}, \tag{30}$$

or in the coefficient form,

$$C_M = M/8\pi\mu\omega_0 ab^2 = a^{-1}(b^2 + c^2)^{\frac{1}{2}}. \tag{31}$$

Two limiting cases are noteworthy. First, when $c \to 0$, and $\beta_0 \to \infty$ such that $c\beta_0 \sim \frac{1}{2}\omega_0 a^3$, as required by (29$a$), the result for the sphere is recovered since by (29c), (28) and (31)

$$b = a, \quad (x^2 + r^2) = a^2, \quad C_M = 1. \tag{32}$$

The other asymptotic case, for $b/a \ll 1$, is especially significant, for the body then resembles an elongated rod. Expansion of (29c) and (31) for small b/a yields

$$\frac{c}{a} = 1 - \frac{b}{2a} - \frac{7}{64}\left(\frac{b}{a}\right)^3 + O\left(\frac{b}{a}\right)^4, \tag{33a}$$

$$C_M = 1 - \frac{b}{2a} + \frac{1}{2}\left(\frac{b}{a}\right)^2 + O\left(\frac{b}{a}\right)^3. \tag{33b}$$

Similarly, the body shape can be deduced from (28):

$$\frac{r_0}{b} = 1 - \left(\frac{b}{c}\right)^2 \frac{x^2(3c^2 - x^2)}{4(c^2 - x^2)^2} + O\left(\frac{b}{c}\right)^4 \quad ((c^2 - x^2) \gg b^2), \tag{34a}$$

$$R_2 = \frac{b}{2}\left[1 - \frac{9}{32}\left(\frac{b}{c}\right)^2 + \frac{1}{64}\left(\frac{b}{c}\right)^3 \cos\theta_2\right] \sec\left(\frac{\theta_2}{2}\right) \quad (R_2 \ll c), \tag{34b}$$

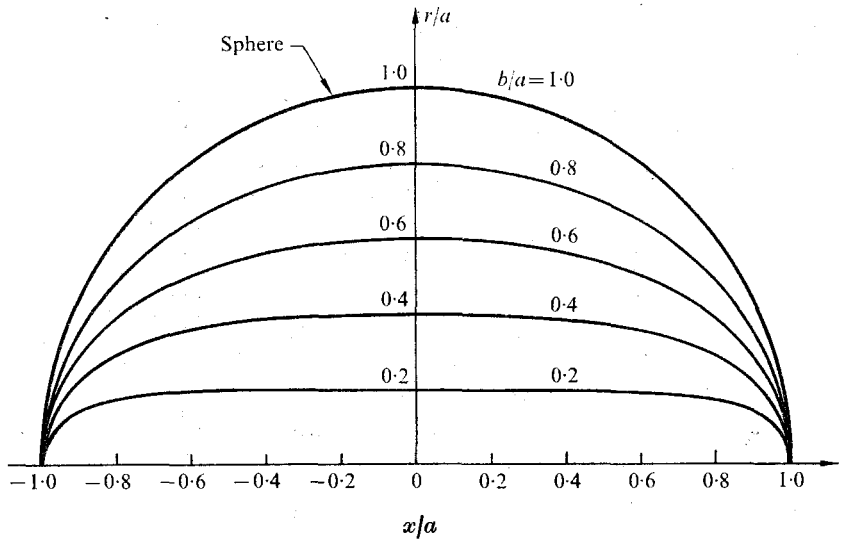

FIGURE 5. A class of axisymmetric bodies represented by a uniform distribution of rotlets, with the sphere and a 'long rod' as limiting cases.

where R_2 is the radial distance from the 'focal point' ($x = c$, $r = 0$), as defined in (22), and $\theta_2 = \tan^{-1}(r/(x-c))$. Thus for b/a small, the central portion of the body (between the foci) is nearly a straight circular cylinder, while the two ends are well rounded, with a local radius of curvature equal to $\frac{4}{3}R_2(\theta_2)$ approximately. These salient features are borne out in the numerical results for $r_0(x)$, as shown in figure 5. The velocity field

$$u_\theta = \beta_0 r B_0(x, r; c) \tag{35a}$$

has near a slender rotator the following asymptotic expansion:

$$u_\theta \sim \frac{\omega_0 b^2}{r}\left(1+\frac{b^2}{c^2}\right)^{\frac{1}{2}}\left[1-\frac{r^2}{2}\frac{x^2+c^2}{(c^2-x^2)^2}+O\left(\frac{cr}{c^2-x^2}\right)^4\right], \tag{35b}$$

$$u_\theta \sim \frac{\omega_0 b^2}{R_2}\left(1+\frac{b^2}{c^2}\right)^{\frac{1}{2}}\tan\left(\frac{\theta_2}{2}\right)\left[1-\left(\frac{R_2}{4c}\cos\frac{\theta_2}{2}\right)^2+O\left(\frac{R_2}{c}\right)^3\right], \tag{35c}$$

indicating that the flow in the central section behaves like a potential vortex, whereas it rotates like a solid body near the axis of symmetry $\theta_2 \ll 1$, $R_2 > (a-c)$. In figure 6 the velocity field given by (35) is plotted in terms of ru_θ as a function of r at several x stations, the slenderness ratio being $b/a = 0{\cdot}1$, which is small enough to represent an elongated body of nearly constant cross-section. It is of interest to note that, near the body mid-section, ru_θ does not vary appreciably with r within a distance of a few body radii, as predicted by (35*b*), and further out u_θ decreases like $(x^2+r^2)^{-1}$, as expected for an equivalent single rotlet. The flow near the two body ends exhibits a behaviour transitional between the two former types of flows. The overall picture indicates that a large volume of the fluid is induced to move with the rotating body.

In the limit as $b/a \to 0$, we deduce from (30) that the torque per unit length of the cylinder is

$$M_{2D} = M/2a = 4\pi\mu\omega_0 b^2. \tag{36}$$

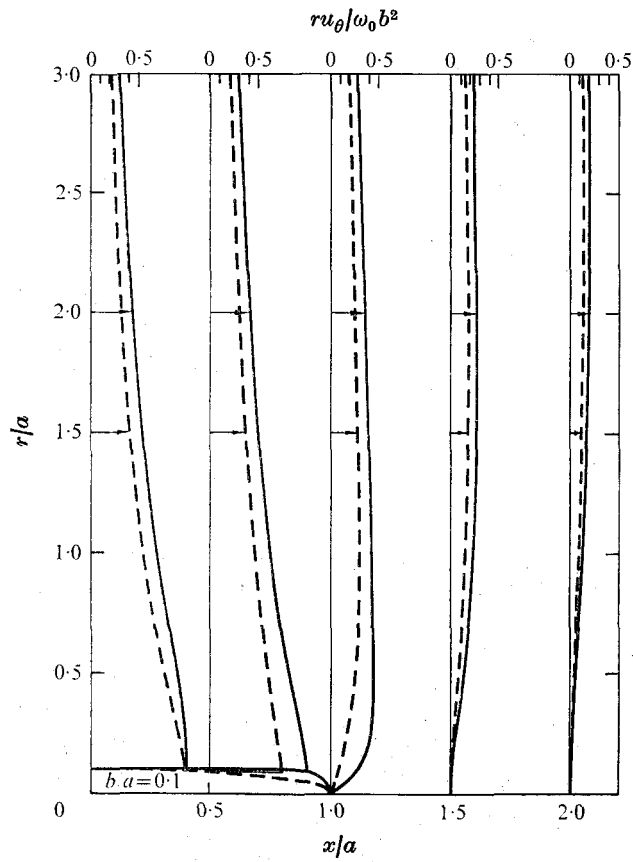

FIGURE 6. Local distributions of the fluid angular momentum ru_θ as functions of x/a and r/a for two shapes of body in rotation: ——, a 'long rod' (with Γ = constant, $-c < x < c$); - - - -, a prolate spheroid; both have the same slenderness ratio $b/a = 0{\cdot}1$. The multiple scales for ru_θ are marked on the top frame line. Note the difference between the slopes of the ru_θ curves for these two cases. The fluid near the x axis off the body rotates like a solid body, and the flow at large distances behaves like that due to a single rotlet.

Both this result and the corresponding velocity u_θ (see equation (35b)) agree with the exact solution of the Navier–Stokes equations for the rotating circular cylinder. A far-reaching interpretation of this finding is now at hand: although we started with the assumption of low Reynolds number for arbitrary shapes, this restriction (on the Reynolds number) becomes decreasingly necessary, so that the range of validity of the theory extends to moderate and even high Reynolds numbers, as the slenderness parameter b/a of the *rotating* body (without translation) decreases. We shall return to this point later (in § 6). It is of basic importance to notice the distinction between the present reduction from three- to two-dimensional *rotating* flows and the classical Stokes paradox for *translational* flows.

For arbitrary b/a, the numerical results for c/a and C_M obtained from (29) and (31) are shown in figure 7. As b/a increases from zero, C_M decreases slightly from its initial value of one to a minimum of 0·883 at $b/a = 0{\cdot}47$, then gradually increases back to one at $b/a = 1$.

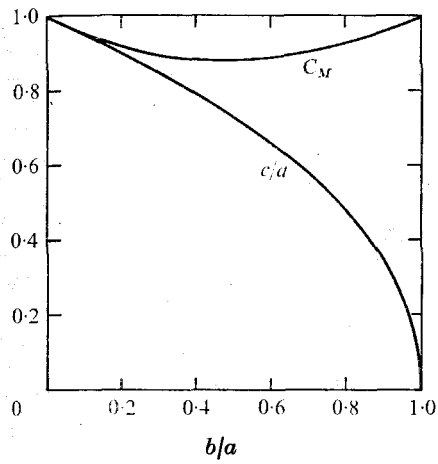

FIGURE 7

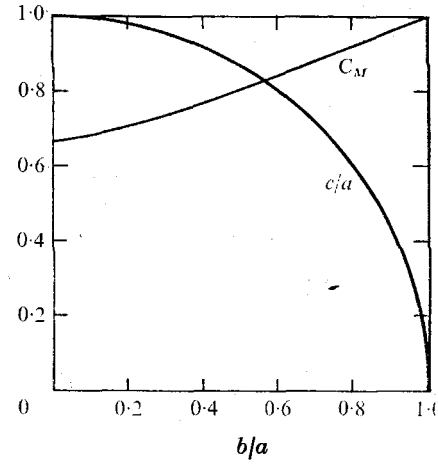

FIGURE 8

FIGURE 7. Variations of the moment coefficient $C_M = M/8\pi\mu\omega_0 ab^2$ and the ratio c/a of the range of rotlet distribution to body length with the slenderness parameter b/a for bodies generated by uniform distributions of rotlets.

FIGURE 8. The moment coefficient $C_M = M/8\pi\mu\omega_0 ab^2$ of rotating prolate spheroids with eccentricity $e = c/a$ (and the ratio of minor to major axis $b/a = (1-e^2)^{\frac{1}{2}}$).

5. Parabolic rotlet distribution: rotating prolate spheroid

Another case of basic interest is the symmetric parabolic distribution

$$\Gamma(x) = \beta_0 + \beta_2 x^2 \quad (|x| \leqslant c), \tag{37}$$

for which the boundary condition (18) now becomes

$$\beta_0 B_0(x, r_0(x); c) + \beta_2 B_2(x, r_0(x); c) = \omega_0 \quad (|x| \leqslant a), \tag{38}$$

where the functions $B_n(x, r; c)$ are defined as

$$B_n(x, r; c) = \int_{-c}^{c} \xi^n R^{-3}(x-\xi, r)\, d\xi \quad (n = 0, 1, 2), \tag{39a}$$

or in the integrated form (B_0 is already given by (28))

$$B_1 = \left(\frac{1}{R_1} - \frac{1}{R_2}\right) + xB_0, \tag{39b}$$

$$B_2 = -\left(\frac{c}{R_1} + \frac{c}{R_2}\right) + xB_1 + \log\frac{R_2 - (x-c)}{R_1 - (x+c)}, \tag{39c}$$

where R_1 and R_2 are given by (22). For the inverse and direct problems (pertaining to a certain class of shape functions) no further discussion is necessary as methods for solving this kind of equation are available. Nevertheless, it is of both theoretical significance and practical value that the following exact solution exists and can be expressed in a closed form.

In an attempt to seek a class of $r_0(x)$ that will reduce the left-hand side of (38) identically to a constant, we first note that the logarithmic term in B_2 (see

equation (39c)) and the remaining part of the algebraic function in (38) must both reduce to constants separately. In fact, the logarithmic function in B_2 will assume a constant value in $-a < x < a$ if and only if the shape function $r = r_0(x)$ belongs to the class of prolate spheroids

$$x^2/a^2 + r^2/b^2 = 1, \tag{40a}$$

where

$$c = ae, \quad b = (1-e^2)^{\frac{1}{2}}a, \tag{40b}$$

with the eccentricity e lying in $0 \leqslant e \leqslant 1$. With the shape function $r_0(x)$ so determined, the left-hand side of (38) becomes independent of x provided that

$$\beta_2 = -\beta_0/c^2. \tag{41}$$

This determines the rotlet distribution (see equation (37)) as

$$\Gamma(x) = \beta_0(1-x^2/c^2) \quad (|x| \leqslant c), \tag{42}$$

which covers the range between the *foci* of the spheroid and vanishes at the end-points $x = \pm c$. Under conditions (40) and (41), (38) finally reduces to

$$\beta_0\left[\frac{2e}{1-e^2} - \log\frac{1+e}{1-e}\right] = \omega_0 c^2, \tag{43}$$

which relates the parameter $\omega_0 a^2/\beta_0$ to the eccentricity of the spheroid and thereby completes our exact solution for the prolate spheroid.

The total torque on the spheroid, by (19) and (42), is

$$M = \tfrac{32}{3}\pi\mu c\beta_0, \tag{44}$$

or in the coefficient form (see (26) for its definition), after making use of (43),

$$C_M = \tfrac{4}{3}e^3[2e - (1-e^2)\log\{(1+e)/(1-e)\}]^{-1}. \tag{45}$$

The velocity field, from (17), is readily found to be

$$u_\theta = \frac{\beta_0}{c^2 r}\left\{(c-x)R_1 + (c+x)R_2 + r^2\log\frac{R_1-(x+c)}{R_2-(x-c)}\right\}, \tag{46}$$

where R_1 and R_2 are given by (22), and β_0 by (43).

The problem of an ellipsoid rotating in a Stokes flow about one of its principal axes was first solved by Edwardes (1892) by means of ellipsoidal harmonics, and was later treated by Jeffery (1922) as a component of the general motion of ellipsoidal particles in suspension. For an ellipsoid of revolution performing an axisymmetric rotation, Jeffery's result (which follows from his equation (36)) becomes

$$L = \frac{16}{3}\frac{\pi\mu\omega_1}{\beta}, \quad \beta \equiv \int_0^\infty \frac{d\lambda}{(a^2+\lambda)^{\frac{1}{2}}(b^2+\lambda)^2}, \tag{47}$$

in the original notation (L being the torque about the x axis, hence our M, and ω_1 being the angular velocity about the x axis, hence our ω_0). Jeffery's solution is found to agree exactly with the C_M given by (45) after the integral in (47) is carried out explicitly. (In Edwardes's result, the numerical factor $\frac{16}{3}$ in (47) is erroneously listed as $\frac{32}{5}$; this error was first pointed out by Gans (1928), who apparently was unaware of Jeffery's (1922) paper.)

The following features of the results are of interest. First, as the eccentricity $e \to 0$, and $\beta_0 \to \infty$ such that $e\beta_0 \sim \frac{3}{4}\omega_0 a^2$ (as dictated by (43)), C_M approaches one, the value for a sphere. On the other hand, as b/a tends to zero (or $e \to 1$), $C_M \to \frac{2}{3}$, which confirms the previous slender-body theory for rotational motions of Chwang & Wu (unpublished research notes), according to which the rectilinear rotlet density for a slender body with local cross-sectional radius $r(x)$ and local axial angular velocity ω_0 is

$$\Gamma(x) = \tfrac{1}{2}\omega_0 r^2(x). \tag{48}$$

Whence, by (19), the torque on a very elongated spheroid ($e \to 1$) is

$$M = 4\pi\mu\omega_0 b^2 \int_{-a}^{a} \left(1 - \frac{x^2}{a^2}\right) dx = \tfrac{16}{3}\pi\mu\omega_0 ab^2, \tag{49}$$

or correspondingly,

$$C_M = \tfrac{2}{3} \quad (\text{as } b/a \to 0). \tag{50}$$

For arbitrary b/a ($\leqslant 1$), the value of C_M, according to (45), increases monotonically from $C_M = \frac{2}{3}$ at $b/a = 0$ to $C_M = 1$ at $b/a = 1$, as shown in figure 8.

For comparison with the previous case of a constant Γ distribution, the velocity u_θ given by (46) is plotted in figure 6 for the same ratio of $b/a = 0{\cdot}1$ as was selected for the long rod. It is of significance to note that even at the mid-section ($x = 0$, $r_0 = b$), where the two body profiles differ by only a negligible amount (see figure 6), the ru_θ curve of the spheroid has a non-zero slope, as opposed to the zero slope of the ru_θ curve for the constant-Γ case. This result implies that the local velocity is appreciably affected by the overall body shape.

Another point of interest concerns the relationship between the focal point at $x = c$ and the radius of curvature of the shape function $r_0(x)$ at the vertex $x = a$. Since the radius of curvature of the spheroid at $x = a$ is $R_a = a(1-e^2)$, and the distance between the vertex and the nearer focal point is $a - c = a(1-e)$, it follows that

$$a - c = \tfrac{1}{2}R_a \quad (\text{for an elongated spheroid}). \tag{51}$$

In comparison, for the case Γ = constant and $b/a \ll 1$ we find (from equation (34*b*)) that

$$a - c = \tfrac{3}{4}R_a \quad (\text{for an elongated 'rod'}). \tag{52}$$

The difference between the factors $\frac{1}{2}$ in (51) and $\frac{3}{4}$ in (52) is actually related to the fact that the rotlet distribution $\Gamma(x)$ vanishes at the terminal points $x = \pm c$ in the former case and $\Gamma(\pm c) \neq 0$ in the latter, as will be shown below.

For arbitrary bodies with well-rounded ends, the general relationship between $a - c$ and R_a may be derived as follows. Confining ourselves to the case of fore-and-aft symmetry for the moment (with $c_1 = c_2 = c$), we can expand the function $F(x, r)$ defined in (18) about the vertex $x = a$, $r = 0$ up to the quadratic terms, giving

$$F(x,r) = F^{(0)} + (x-a)F_x^{(0)} + \tfrac{1}{2}(x-a)^2 F_{xx}^{(0)} + \tfrac{1}{2}r^2 F_{rr}^{(0)} + \ldots, \tag{53a}$$

where

$$F^{(0)} \equiv F(a,0) = \int_{-c}^{c} \frac{\Gamma(\xi)\,d\xi}{(a-\xi)^3}, \quad F_x^{(0)} = -3\int_{-c}^{c} \frac{\Gamma(\xi)\,d\xi}{(a-\xi)^4}, \tag{53b}$$

$$F_{xx}^{(0)} = -4F_{rr}^{(0)} = 12\int_{-c}^{c} \frac{\Gamma(\xi)\,d\xi}{(a-\xi)^5}. \tag{53c}$$

In (53a) the terms odd in r drop out since $F^{(0)}_r = F^{(0)}_{rx} = 0$ on account of $F(x, r$ being even in r. Upon combining (18) and (53a), noting that $F^{(0)} = \omega_0$ as required by the end condition at $x = a, r = 0$, there results for the shape function $r = r_0(x)$ near the end $x = a, r = 0$ the expansion

$$r_0^2(x) = 2R_a(a-x) + 4(a-x)^2 + O((a-x)^3), \tag{54a}$$

where

$$R_a = F^{(0)}_x / F^{(0)}_{rr} = \int_{-c}^{c} \frac{\Gamma(\xi)\, d\xi}{(a-\xi)^4} \Big/ \int_{-c}^{c} \frac{\Gamma(\xi)\, d\xi}{(a-\xi)^5} \tag{54b}$$

is the radius of curvature of $r_0(x)$ at $x = a$. For very elongated bodies, $a - c \ll a$, the asymptotic expansions of the integrals in (54b) (by appropriate successive integrations by parts) yield

$$\frac{R_a}{a-c} = \left(\frac{4}{3}\right) \frac{\Gamma(c) - \frac{1}{2}(a-c)\,\Gamma'(c) + \frac{1}{2}(a-c)^2\,\Gamma''(c) + o((a-c)^2)}{\Gamma(c) - \frac{1}{3}(a-c)\,\Gamma'(c) + \frac{1}{6}(a-c)^2\,\Gamma''(c) + O((a-c)^3)}, \tag{55}$$

in which the primes denote differentiation. It is readily seen that (55) reduces to (51) and (52) in the respective cases. For bodies not having fore-and-aft symmetry, (55) is also applicable to the left end at $x = -a$ provided that $a - c$ in (55) is replaced by $a - c_1$ and $\Gamma^{(n)}(c)$ by $\Gamma^{(n)}(-c_1)$.

The above result, (54) and (55), also suggests that a representation of the class of bodies of revolution with pointed ends (i.e. $|dr_0/dx| < \infty$ and $R_a = 0$ at $x = a$) can be arrived at by setting $c = a$ and requiring $\Gamma(x)$ to vanish like $(x-a)^3$ at $x = a$ so as to ensure the convergence of all the integrals involved.

For arbitrary axisymmetric body forms, one may apply known numerical methods to solve the integral equation (18) for the distribution function $\Gamma(x)$ and parameters c_1 and c_2. A specific collocation method may be employed by first assuming for $\Gamma(x)$ a polynomial distribution

$$\Gamma(x) = \sum_{n=0}^{N} \beta_n x^n \quad (-c_1 \leqslant x \leqslant c_2). \tag{56}$$

(For bodies with fore-and-aft symmetry we omit the terms with odd powers of x and set $c_1 = c_2 = c$.) Equation (18) then becomes

$$\sum_{n=0}^{N} \beta_n B_n(x, r_0(x); c_1, c_2) = \omega_0 \quad (|x| \leqslant a), \tag{57}$$

where $B_n(x, r; c_1, c_2)$ is defined by (39a) with the limits of integration suitably modified (to $-c_1$ and c_2). Thus, (57) provides the implicit solution for $r_0(x)$ for the inverse problem when the parameters $\beta_0, \beta_1, \ldots, \beta_N$, c_1 and c_2 are given. For the direct problem, with the shape function $r_0(x)$ prescribed, the $N+3$ unknowns $\beta_0, \beta_1, \ldots, \beta_N, c_1$ and c_2 may be determined by the collocation method after $N+3$ points x_m, with $-a = x_0 < x_1 < x_2 < \ldots < x_{N+2} = a$, have been appropriately chosen for invoking (57). The total torque on the axisymmetric body is then given by (19) and (56). We shall not, however, pursue this general case any further here.

6. Effects of body slenderness on the limitation of low Reynolds number

It remains for us to verify whether the assumption that inertia forces can be neglected is actually self-consistent, that is, if in the Navier–Stokes equation

$$\rho\mathbf{u}.\nabla\mathbf{u}+\nabla p=\mu\nabla^2\mathbf{u}+4\pi\mu\nabla\times\boldsymbol{\Omega} \tag{58}$$

the inertia force $\rho\mathbf{u}.\nabla\mathbf{u}$ can always be neglected uniformly in the flow field when the Reynolds number is small and when only solenoidal forcing functions are present. According to the present solution (17), the velocity at sufficiently large distances behaves like a single rotlet, that is

$$\mathbf{u}=\mathbf{e}_\theta u_\theta,\quad u_\theta\sim\omega_0 a_0^3 r/R^3, \tag{59a}$$

where $R^2=x^2+r^2$ and a_0 is the equivalent sphere radius given by

$$\int_{-c_1}^{c_2}\Gamma(\xi)\,d\xi=\omega_0 a_0^3. \tag{59b}$$

The inertia force term $\rho\mathbf{u}.\nabla\mathbf{u}=\rho(u_\theta/r)\,\partial(\mathbf{e}_\theta u_\theta)/\partial\theta$ is of order $\rho(\omega_0 a_0^3)^2/R^5$, and an estimate of the viscous force $\mu\nabla^2\mathbf{u}$ is $\mu\omega_0 a_0^3/R^4$. Thus the ratio of the order of magnitude of the neglected inertia force to that of the retained viscous force is

$$\frac{|\rho\mathbf{u}.\nabla\mathbf{u}|}{|\mu\nabla^2\mathbf{u}|}=\frac{\Omega_0 a_0^2}{\nu}\frac{a_0}{R}=Re\left(\frac{a_0}{R}\right). \tag{60}$$

This ratio is everywhere small, at distances $R\sim O(a_0)$ or greater, as long as the Reynolds number $Re\ll 1$.

In the vicinity of an *elongated* body, the above ratio of forces is further influenced by the body geometry, as we have noted earlier. To examine more critically this point, especially in connexion with relaxing the restriction on the Reynolds number to small values, we rewrite (58) as

$$\rho\boldsymbol{\omega}\times\mathbf{u}+\nabla(\tfrac{1}{2}\rho u^2+p)=\mu\nabla^2\mathbf{u}+4\pi\mu\nabla\times\boldsymbol{\Omega}. \tag{61}$$

The present solution (which always makes the right-hand side of (61) vanish, see (7)) will remain a good approximation as long as the corresponding value of $\rho\boldsymbol{\omega}\times\mathbf{u}$ is small relative to the order of magnitude of the viscous force $\mu\nabla^2\mathbf{u}$ since when this condition is satisfied we can always adjust the pressure by taking

$$p+\tfrac{1}{2}\rho u^2=\text{constant} \tag{62}$$

rather than (5). Now, from the general solution (17) it follows that

$$\boldsymbol{\omega}\times\mathbf{u}=-\mathbf{e}_x\frac{\partial}{\partial x}(\tfrac{1}{2}u_\theta^2)-\mathbf{e}_r\frac{u_\theta}{r}\frac{\partial}{\partial r}(ru_\theta).$$

For very slender bodies, ru_θ has been noted (see equation (35*b*)) to be nearly a constant function of r in a neighbourhood of the body. Consequently, an estimate of the term $\rho\boldsymbol{\omega}\times\mathbf{u}$ is $\partial(\rho u_\theta^2)/\partial x$, or $\rho u_\theta^2/a$, where $2a$ is the length of the elongated body (with slenderness parameter $\epsilon=b/a\ll 1$). Further, the viscous

force $\mu\nabla^2\mathbf{u}$ is seen to be of order $(\mu u_\theta/b^2)(1+O(\epsilon^2))$. Thus, the ratio of the term $\rho\boldsymbol{\omega}\times\mathbf{u}$ to the viscous force becomes, in the neighbourhood of an elongated body,

$$|\rho\boldsymbol{\omega}\times\mathbf{u}|/|\mu\nabla^2\mathbf{u}| = \left(\frac{\rho u_\theta^2}{a}\right)\Big/\left(\frac{\mu u_\theta}{b^2}\right) = \frac{u_\theta b}{\nu}\left(\frac{b}{a}\right) = \epsilon\, Re. \tag{63}$$

This shows that the present solution will hold, and any significant inertial effect can be incorporated with the pressure field by (62), if

$$Re \ll 1/\epsilon. \tag{64}$$

The upper bound $Re^* = 1/\epsilon$ of the Reynolds-number range can be large for $\epsilon \ll 1$. This explains the previous observation that the present solution for the flow near an elongated rod actually has a range of validity extending to higher values of the Reynolds number.

This work was partially sponsored by the National Science Foundation, under Grant GK 31161X, and by the Office of Naval Research, under Contract N00014-67-A-0094-0012.

REFERENCES

Batchelor, G. K. 1967 *An Introduction to Fluid Dynamics*. Cambridge University Press.

Batchelor, G. K. 1970 Stress system in a suspension of force-free particles. *J. Fluid Mech.* **41**, 545–570.

Blake, J. R. & Chwang, A. T. 1974 Fundamental singularities of viscous flow. Part 1. The image system in the vicinity of a stationary no-slip boundary. *J. Eng. Math.* **8**, 23–29.

Chwang, A. T. & Wu, T. Y. 1971 A note on the helical movement of micro-organisms. *Proc. Roy. Soc.* B **178**, 327–346.

Chwang, A. T. & Wu, T. Y. 1974 Helical movement of cylindrical tails in self-propelling micro-organisms. To be published.

Edwardes, D. 1892 Steady motion of a viscous liquid in which an ellipsoid is constrained to rotate about a principal axis. *Quart. J. Math.* **26**, 70–78.

Gans, R. 1928 Zur Theorie der Brownschen Molekularbewegung. *Ann. Phys.* **86**, 628–656.

Gray, J. & Hancock, G. J. 1955 The propulsion of sea-urchin spermatozoa. *J. Exp. Biol.* **32**, 802–814.

Hancock, G. J. 1953 The self-propulsion of microscopic organisms through liquids. *Proc. Roy. Soc.* A **217**, 96–121.

Happel, J. & Brenner, H. 1965 *Low Reynolds Number Hydrodynamics*. Prentice-Hall.

Jeffery, G. B. 1922 The motion of ellipsoidal particles immersed in a viscous fluid. *Proc. Roy. Soc.* A **102**, 161–179.

Kellogg, O. D. 1929 *Foundations of Potential Theory*. New York: Murray Printing Co.

Lagerstrom, P. A. 1964 Laminar flow theory. In *Theory of Laminar Flows* (ed. F. K. Moore), vol. IV. *High Speed Aerodynamics and Jet Propulsion*, §B. Princeton University Press.

Lamb, H. 1932 *Hydrodynamics*. Cambridge University Press.

Lighthill, M. J. 1969 Hydromechanics of aquatic animal propulsion. *Ann. Rev. Fluid Mech.* **1**, 413–445.

Oseen, C. W. 1927 *Neuere Methoden und Ergebnisse in der Hydrodynamik*. Leipzig: Akad. Verlagsgesellschaft.